Supplementary Material

Supplementary Figures

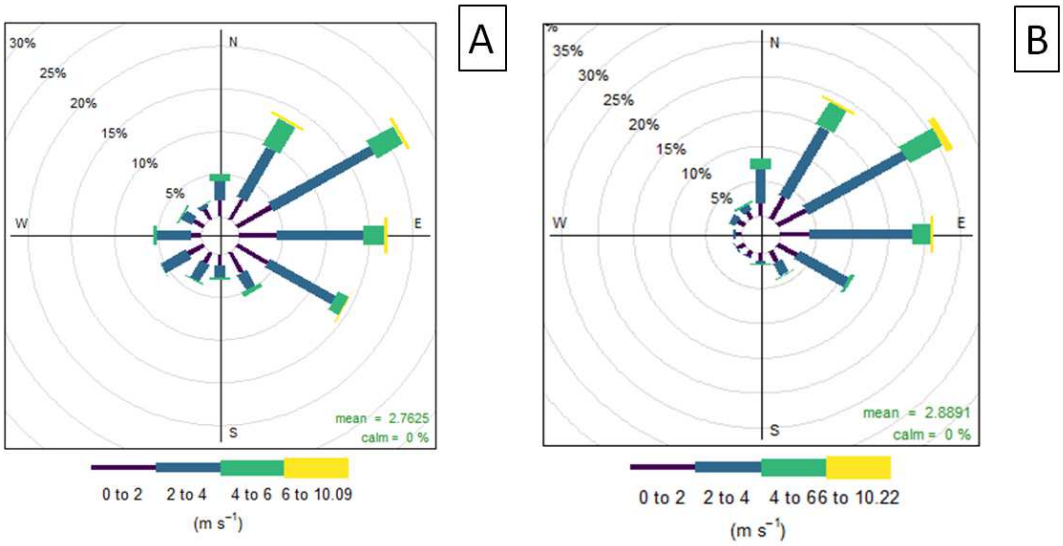

Supplementary Figure 1. Wind roses for the dry season (A) and wet season (B) sampling days. The scale reports the frequency of counts by wind direction (%), whereas the angle represents the wind direction and the radius the wind speed.

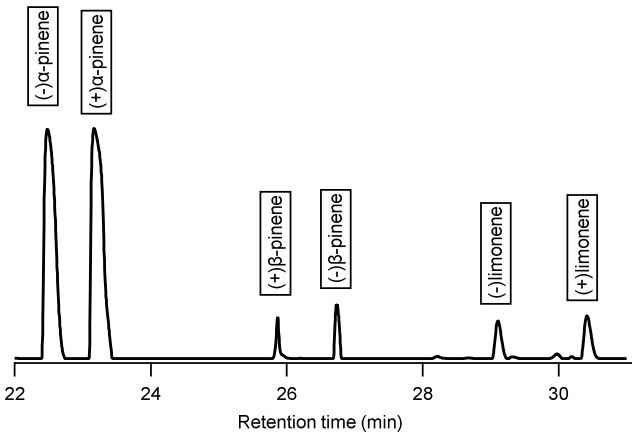

Supplementary Figure 2. Example of chromatogram showing the separation of chiral compounds from a gas mixture including (-)-α-pinene, (+)-α-pinene, (+)-β-pinene, (-)-β-pinene, (-)limonene, (+)limonene achieved by using a β-cyclodextrin based column.

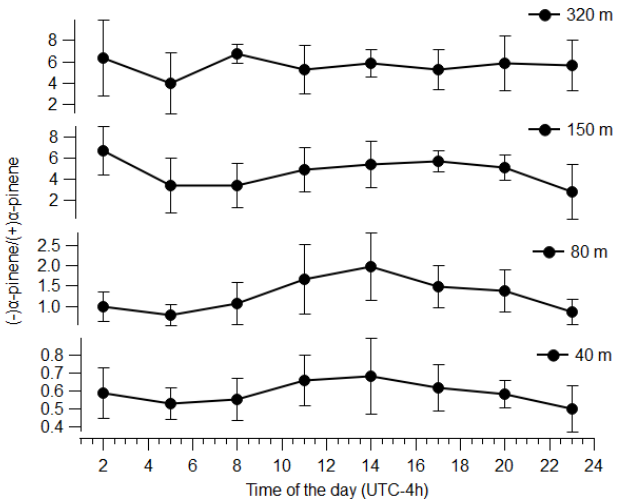

Supplementary Figure 3. Chiral ratio (reported as ((-)-α-pinene/(+)-α-pinene)) measured during the dry season at 40 m, 80 m, 150 m and 320 m from the tower ATTO. Data points show averaged values for different sampling times across the whole collected data set. Error bars represent the standard deviation of the data set. The number of samples taken and variability during sampling days can be seen in Fig. 4 of the manuscript.

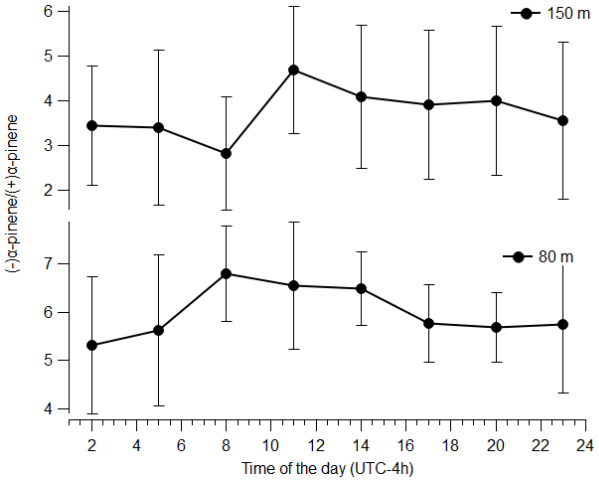

Supplementary Figure 4. Chiral ratio (reported as ((-)-α-pinene/(+)-α-pinene)) measured during the wet season at 80 m and 150 m from the tower ATTO. Data points show averaged values for different sampling times across the whole collected data set. Error bars represent the standard deviation of the data set. The number of samples taken and variability during sampling days can be seen in Fig. 5 of the manuscript.

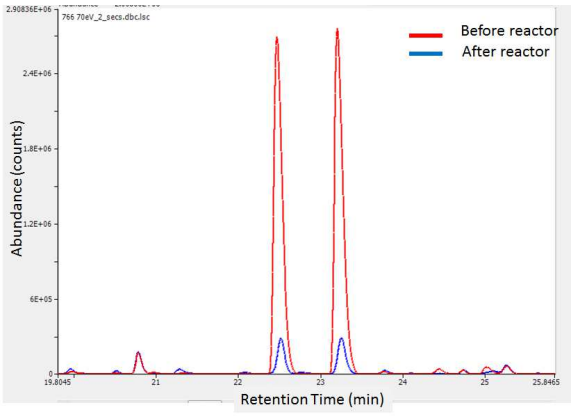

Supplementary Figure 5. Chromatograms of samples collected before reactor (racemic mixture of α-pinene diluted in synthetic air, ~1 ppbv concentration) and after reactor (racemic mixture of α-pinene diluted in synthetic air and mixed with OH and O_3 generated in situ). The peaks eluting at 22.6 min and 23.3 min correspond respectively to (-)-α-pinene and (+)-α-pinene.

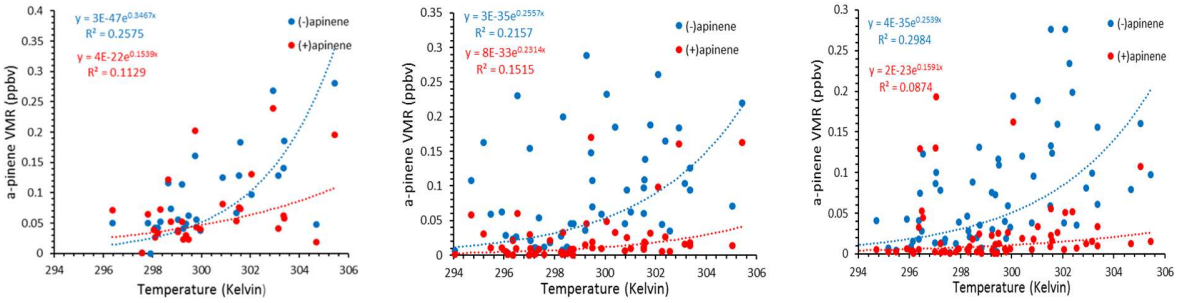

Supplementary Figure 6. Dry season ambient air mixing ratios of (-)-α-pinene and (+)-α-pinene and temperature measured at 80 m (A), 150 m (B) and 320 m (C). Temperature was monitored at 80 m from the INSTANT tower (~150 m from ATTO tower).

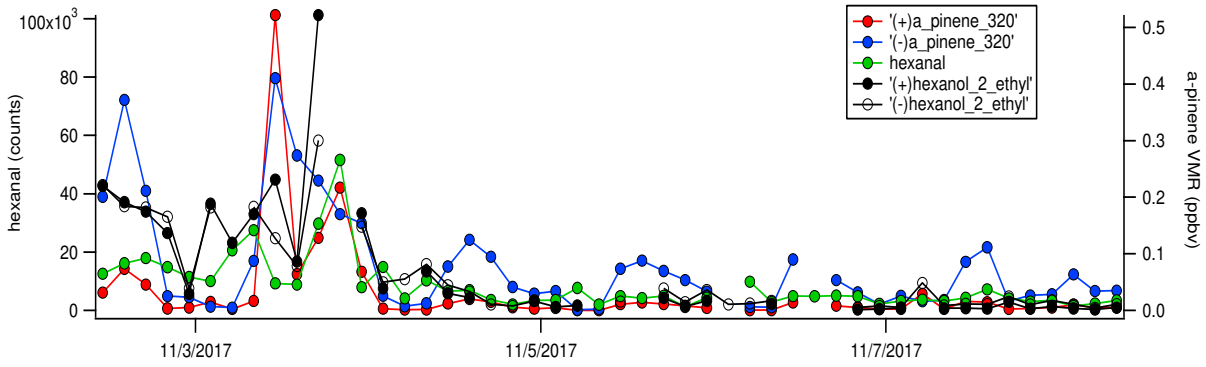

Supplementary Figure 7. Peak areas counts (hexanal and hexanols) and volume mixing ratio (α-pinene) measured from the ATTO tower at 320 m during the dry season 2017.

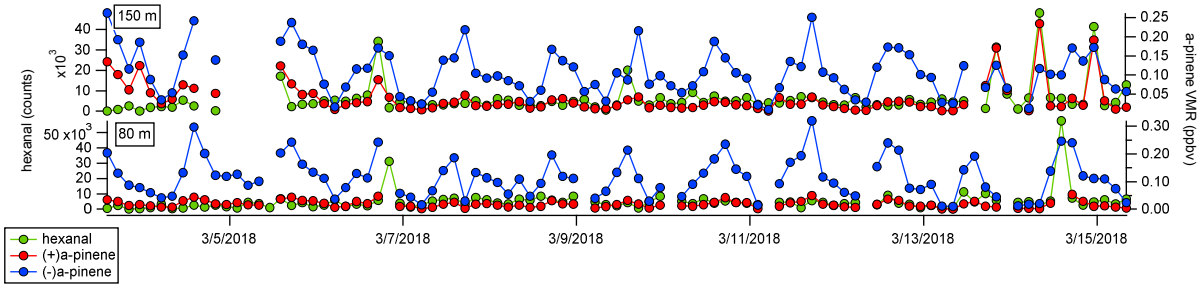

Supplementary Figure 8. Peak area counts (hexanal) and volume mixing ratio (α-pinene) measured at 80 m and 150 m during the wet season 2018.

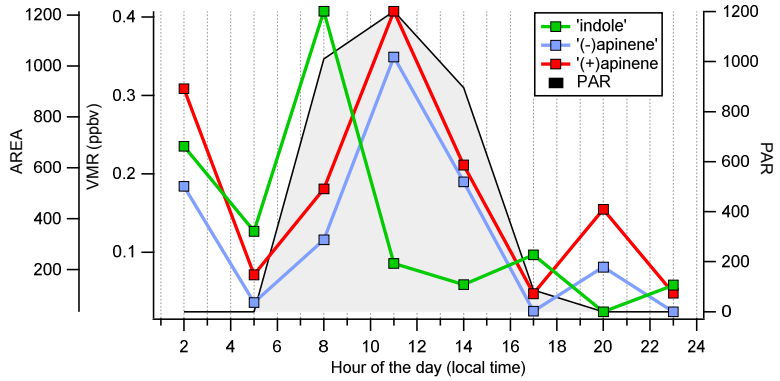

Supplementary Figure 9. Counts of peak area (indole), volume mixing ratio (α-pinene) and photosynthetic active radiation measured during the dry season 2017 at 40 m on the ATTO tower. Data of photosynthetic active radiation (PAR) were collected from the neighboring INSTANT tower.

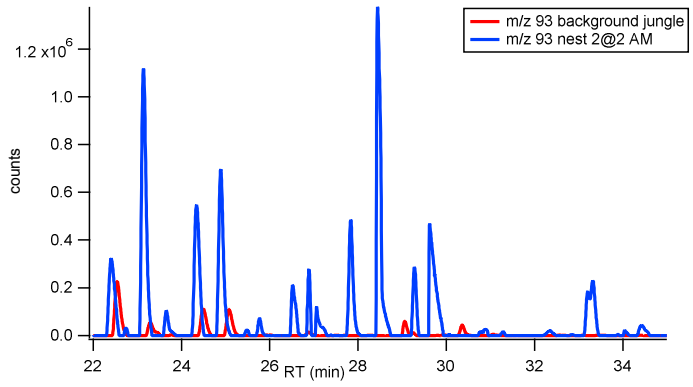

Supplementary Figure 10. Extracted ion chromatogram areas comparison between one sample taken during night above a termite nest (blue) and one sample taken during the afternoon of the background jungle (red). The background jungle sample was taken by moving the same sampling inlet a few meters away from the termite nest, and by installing it at some distance from trees, leaves, litter, bark. The peaks eluting at 22.6 min and 23.3 min correspond respectively to (-)-α-pinene and (+)-α-pinene.

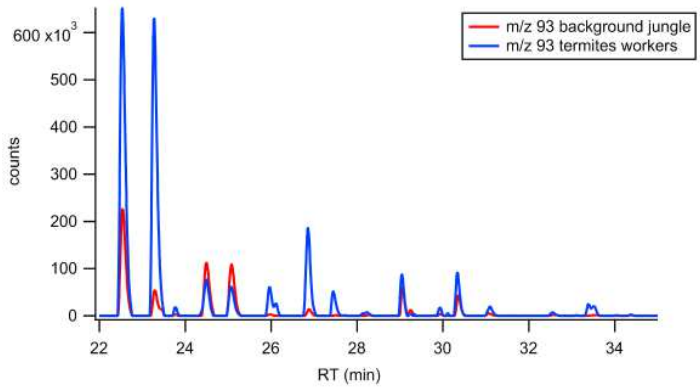

Supplementary Figure 11. Extracted ion chromatogram areas comparison between one sample taken above a walking line of termite soldiers and workers (blue) and one sample taken during the afternoon of the background jungle (red). The background jungle sample was taken by moving the same sampling inlet a few meters away from the termite nest, and by installing it at some distance from trees, leaves, litter, bark. The peaks eluting at 22.6 min and 23.3 min correspond respectively to (-)-α-pinene and (+)-α-pinene.

Supplementary Notes, Discussion, Methods

Wind direction and speed for the days of sampling during November 2017 (A) and March 2018 (B) are reported as wind roses in Supplementary Figure 1. The two sampling seasons do not show significant differ in wind direction and speed.

The separation and resolution achieved by the method and analytical technique used permits to distinguish unambiguously three main pair of chiral molecules: α-pinene, β-pinene and limonene (Supplementary Figure 2).

Averaged campaign values of the chiral ratio reported as (-)-α-pinene/(+)-α-pinene for different times of the day are shown in Supplementary figures 3 (dry season 2017) and 4 (wet season 2018). Error bars represent the standard deviation calculated for the whole data set. The chiral ratio is close to 1, with a diel profile reporting dominance of (-)-α-pinene during the day, and dominance of (+)-α-pinene during the night, at 80 m during the dry season. In all the other cases, either (+)-α-pinene (40 m dry season), either (-)-α-pinene (150 m, 320 dry season and 80 m, 150 m wet season) are significantly dominant.

Since gas phase reactions are relatively high energy interactions it is not expected that a chirally selective reaction could occur in the gas phase. Schneider et al. (1996) saw no chiral selectivity in measurement of alkyl nitrates which are products formed in the gas phase. A simple test was performed to see if atmospheric oxidants such as the hydroxyl radical (OH) and ozone (O3) can selectively react with a racemic mixture of α-pinene, by using the same instrumentation and analysis employed for ambient samples discussed in the manuscript. Supplementary Figure 5,

shows the peak areas of the chromatograms of the samples collected before the reactor (racemic mixture of α-pinene diluted in synthetic air, concentration ~ 1 ppbv) and after the reactor (racemic mixture of α-pinene diluted in synthetic air, mixed with OH and O3 generated in situ). Note the concentrations of OH and ozone are much higher than ambient in order to amplify any effect present. The measured peak areas quantified before the reactor were $2.3x10^7$ and $2.4x10^7$ counts respectively for (-)-α-pinene and (+)-α-pinene (48% and 49% the total α-pinene), while they reduced to 2.4 $x10^6$ and 2.42 $x10^6$ counts after the reactor (47% and 48% the total α-pinene). Full details on the experiments are given in the method section.

Mixing ratios (VMR) of α-pinene enantiomers were plotted against temperature for all samples taken during the dry season at 80 m (panel A, Fig.6), at 150 m (panel B, Fig.6), and 320 m (panel C, Fig.6). Similar trends as for the wet season data (Fig. 6 manuscript) are observed.

Tracers of trees mechanical damage as GLVs (green leaf volatiles) were observed to increase at the same time or slightly before the increase of α-pinene, and specifically (+)-α-pinene at any height and season (Supplementary Figures 7 and 8).

Indole is analysed in quality of tracer for herbivore induced terpenes emissions (see main text for references of indole acting as a primer). Diel profiles of indole and terpenes at 40m suggest a connection in their emissions from the local canopy (Supplementary Fig. 9).

Sampling above two termites nests conducted during September 2019 highlighted the influence of insects on terpenes emissions. As the two chromatograms comparisons reported in Supplementary Figures 10 and 11 indicate, the signal of (+)-α-pinene (23.3 min) is enormously enhanced when compared to background forest air, which is instead characterized by a large signal of (-)-α-pinene (22.6 min).

An approximate calculation of the flux rate for (+)-α-pinene has been made assuming the termite nest behaves as an enclosure. Details of the sampling are reported in the method section in the manuscript. We considered all the data of (+)-α-pinene obtained from the 75 samples collected outside two nests selected at the ATTO site. In order to differentiate background air samples from nest samples we considered the dependence of the chiral ratio on the total ion chromatogram integrated area. With this approach we could identify 2 clusters of samples, which were used to determine an average concentration of (+)-α-pinene for the nest and an average concentration of (+)-α-pinene for the background forest air. Assuming the nest behaves as an enclosure, we considered the former as the concentration entering the enclosure (C_{in}), and the latter as the concentration exiting the enclosure (C_{out}), with mass being the mass of termites in the nest and flow the sampling flow used (L/h) to calculate the emission rate (ER):

$$ER = \frac{flow}{mass} \text{ x } (C_{out}\text{-}C_{in})$$

Based on the characteristics of the sampled nests in ATTO (hemielliptic shape with its base on the tree surface) we considered the colony biomass (g) dependence on nest volume as reported in Pequeño et al.[50] for similar nest types. Therefore, a colony biomass value was determined based on the measured volume of the sampled nests and used to calculate ER. This value was then upscaled considering the nest population per hectare in the Amazon rainforest reported by Martius et al.[51]. It is important to note that this estimate is approximate, for the following reasons: first, it is based

on the assumption that the nest behaves as an enclosure flushed with background forest air, while a rigorous study should use a clean enclosure with isolated insects flushed with VOC free air; second, although few exemplars of termites were collected for identification, here the colony biomass was determined based on corresponding characteristics of sampled termites nests available in literature. Moreover, the nest population per hectare in the Amazon rainforest reported by Martius was estimated in 1994, therefore changes due to deforestation and increasing drought in the Amazons may have impacted such estimate as well.

References

Schneider M. and Ballschmiter K., Separation of Diastereomeric and Enantiomeric Alkyl Nitrates-Systematic Approach to Chiral Discrimination on Cyclodextrin LIPODEX-D. 2, 5, Chem. Eur. J. 1996.